

RESEARCH

Open Access

# NHERF1/EBP50 is an organizer of polarity structures and a diagnostic marker in ependymoma

Maria-Magdalena Georgescu<sup>1,2\*</sup>, Paul Yell<sup>1</sup>, Bret C Mobley<sup>3</sup>, Ping Shang<sup>1</sup>, Theodora Georgescu<sup>2</sup>, Shih-Hsiu J Wang<sup>4</sup>, Peter Canoll<sup>4</sup>, Kimmo J Hatanpaa<sup>1</sup>, Charles L White III<sup>1</sup> and Jack M Raisanen<sup>1</sup>

## Abstract

NHERF1/EBP50, an adaptor protein required for epithelial morphogenesis, has been implicated in the progression of various human malignancies. *NHERF1*-deficient mice have intestinal brush border structural defects and we report here that they also have disorganized ependymal cilia with development of non-obstructive hydrocephalus. Examination of mouse and human brain tissues revealed highest NHERF1 expression at the apical plasma membrane of ependymal cells. In ependymal tumors, NHERF1 expression was retained in polarized membrane structures, such as microlumens, rosettes and canals, where it co-localized with some of its ligands, such as moesin and PTEN. Analysis of a comprehensive panel of 113 tumors showed robust NHERF1 labeling of microlumens in 100% of ependymomas, subependymomas, and pediatric anaplastic ependymomas, and in 67% of adult anaplastic ependymomas. NHERF1 staining was present in 35% of ependymoma cases that lacked reactivity for EMA, the routine immunohistochemical marker used for ependymoma diagnosis. NHERF1 labeling of microlumens was either absent or rarely seen in other types of brain tumors analyzed, denoting NHERF1 as a reliable diagnostic marker of ependymal tumors. Anaplastic foci and a subset of adult anaplastic ependymomas showed complete absence of NHERF1-labeled polarity structures, consistent with a loss of differentiation in these aggressive tumors. These data highlight a role for NHERF1 in ependymal morphogenesis with direct application to the diagnosis of ependymal tumors.

**Keywords:** NHERF1/EBP50, Ependymoma, Hydrocephalus, Polarity, Moesin, PTEN

## Introduction

In the development of the central nervous system (CNS), ependymal cells arise from the asymmetric division of radial glia, the polarized precursor cells spanning the central canal to the pia mater [1,2]. Ependymal cells are terminally differentiated glial cells that line the ventricular system and retain the polarity of their precursors. Arranged as a single layer of cuboidal cells with adherens junctions, basally located nuclei and specialized apical plasma membrane (PM) containing cilia and microvilli, they resemble epithelial cells forming glandular lumens except for the lack of a well-defined basement membrane.

Ependymal cells form the cerebrospinal fluid (CSF)-brain barrier and, through the unidirectional beat of their cilia, they direct the flow of the CSF in the ventricular system. Pathologically, structural alterations of the ependymal cilia may lead to hydrocephalus development [3], whereas the uncontrolled proliferation of ependymal cells or their precursors results in the growth of generally non-infiltrative glial ependymal tumors. Depending on their mitotic rate, ependymal tumors fall into three categories, in increasing order of aggressiveness: subependymomas (WHO grade I), ependymomas (WHO grade II) and anaplastic ependymomas (WHO grade III). Whereas subependymomas occur in adults and have a benign course, higher grade tumors are more likely to arise in childhood where overall 5-year survival rates of 60% are seen [4]. These rates have not improved significantly in the past 40 years due to lack of effective chemotherapy and a poor understanding of tumor pathogenesis [5].

\* Correspondence: maria-magdalena.georgescu@phhs.org

<sup>1</sup>Department of Pathology, The University of Texas Southwestern Medical Center, Dallas, TX 75390, USA

<sup>2</sup>Department of Neuro-Oncology, The University of Texas MD Anderson Cancer Center, Houston, TX 77030, USA

Full list of author information is available at the end of the article

NHERF1/EBP50 (Na<sup>+</sup>/H<sup>+</sup> exchanger 3 regulating factor 1; ezrin-radixin-moesin (ERM) binding phosphoprotein 50) is an adaptor protein localized mainly at the apical PM in human epithelia [6]. NHERF1 interacts with the ERM-NF2 (neurofibromatosis 2) cytoskeletal proteins via its carboxyl (C)-terminal ERM-binding region and with many ligands, including PTEN tumor suppressor and platelet-derived growth factor receptor (PDGFR), via its amino (N)-terminal tandem PDZ (PSD95-Dlg1-ZO1) domains [7,8]. NHERF1 behaves as a tumor and epithelial-to-mesenchymal transition suppressor in cultured cells, through its effects on PTEN and  $\beta$ -catenin [9-11], and is required for gland morphogenesis with lumen formation in three-dimensional polarized epithelium [12]. Importantly, NHERF1 overall loss or PM displacement has been reported in aggressive tumors, including carcinomas and glioblastoma [9,13,14]. *NHERF1* knockout mice have ultrastructural defects of the intestinal apical brush border membrane and of the cochlear outer hair cell cilia bundles [15,16]. Prompted by the observation that these mice also develop non-obstructive hydrocephalus, we mapped the highest NHERF1 expression in the CNS at the specialized apical PM of ependymal cells. The immunohistochemical of ependymal tumors showed a unique expression of NHERF1 and some NHERF1-associated molecules, such as moesin, in microlumens that represent precursor polarized membrane structures retained by neoplastic ependymal cells. Besides this robust and specific NHERF1 expression that we propose as a diagnostic marker for these tumors, a gradual loss of NHERF1 was observed in anaplastic ependymomas, compatible with a previously demonstrated tumor suppressor role for NHERF1.

## Materials and methods

### Animals

The *NHERF1*-deficient mice were inbred for 10 generations in C57BL/6J background and genotyped as described [16]. Newborn mice were observed regularly for skull deformity or signs of neurological impairment. When skull deformity was present, mice were sacrificed and the skulls were dissected and grossly examined by serial sectioning following decalcification. To assess the incidence of subclinical hydrocephalus, whole litters of 5 week-old progeny from *NHERF1* heterozygous parents were examined as above. All experiments were performed under approved MD Anderson Cancer Center IACUC protocols.

### Mouse tissue histology and immunostaining

Brains were fixed overnight in 10% formalin, embedded in paraffin and 4 $\mu$ m sections were processed for hematoxylin and eosin (H&E) staining as described [16]. The immunofluorescence analysis was performed as described [11] with NHERF1 1:300 (Abcam, Cambridge, MA),  $\beta$ -catenin 1:500

and acetylated  $\alpha$ -tubulin 1:1000 (Sigma-Aldrich, St Louis, MO) primary antibodies. Image stacks were acquired with a Zeiss Axiovert 200M inverted microscope (Carl Zeiss MicroImaging, Thornwood, NY) and deconvolved with AxioVision Rel 4.5 SP1 software.

### Human specimens, histology and electron microscopy

Brain tumor resection or biopsy specimens were obtained from the Division of Neuropathology University of Texas Southwestern Medical Center, Dallas, TX, Division of Neuropathology, Columbia University, New York, NY and Department of Pathology, Vanderbilt University, Nashville, TN. The specimens were processed for H&E staining or immunohistochemistry (IHC) [17], with antibodies for NHERF1 1:3200 (Thermo/Fisher, Waltham, MA), moesin 1:100, PTEN 1:100 and PDGFR $\alpha$  1:100 (Cell Signaling Technology, Danvers, MA), NF2 1:200 and YAP1 1:200 (Santa Cruz Biotechnology, Santa Cruz, CA),  $\beta$ -catenin 1:1600 (Invitrogen, Carlsbad, CA), EGFR 1:1000 and EMA 1:400 (Dako, Carpinteria, CA), and PHLPP2 1:100 (Bethyl Laboratories, Montgomery, TX).

### Statistical analysis and scan imaging

Images were acquired at 20x magnification, and where specified, at 40x magnification, with Aperio Scanscope CS2 whole slide image system (Leica Biosystems, San Diego, CA), analyzed by ImageScope software, version 12.1.0.5029, and quantified using the Nuclear algorithm, version 11.2. Three tumor areas were analyzed from each slide. When multiple tumor fragments were present, areas from 3 different fragments were chosen. The Nuclear algorithm was fine-tuned for object recognition, including intensity thresholds, edge trimming of objects and smoothing/declustering of nuclei/lumens, in order to obtain the primary output represented by the number of positive lumens and number of negative nuclei. Numerical data were examined for normality of distribution and expressed as mean  $\pm$  SEM by using the GraphPad Prism program (GraphPad Software, La Jolla, CA). Two-tailed t-test with Welch's correction for variances significantly different was used to analyze the differences between groups. Statistical significance was considered for  $P < 0.05$ . Confidence intervals for all tests were 95%.

## Results

### *NHERF1*-deficient mice develop hydrocephalus

We and others have characterized a series of morphological and phenotypical alterations in *NHERF1*-deficient mice that include phosphate reabsorption impairment, altered intestinal brush border membrane, lack of development of the lobuloalveolar lactating mammary gland and abnormalities of cochlear cilia bundles with hearing defects [15,16,18,19].

A proportion of *NHERF1*-deficient mice also showed dilatation of the lateral, 3rd and 4th ventricles of the brain that define non-obstructive hydrocephalus (Figure 1A-B). The degree of hydrocephalus varied from overt forms, in which skull deformity and severe developmental impairment were present (Figure 1A), to clinically inapparent forms, in which mild to moderate dilatation

of the ventricles was observed after skull dissection and brain sectioning (Additional file 1: Figure S1A). Whereas overt forms were sporadic, the dissection of several litters generated from *NHERF1* heterozygous parents showed a variable penetrance of the mild phenotype with rates up to 100% (Additional file 1: Figure S1B).

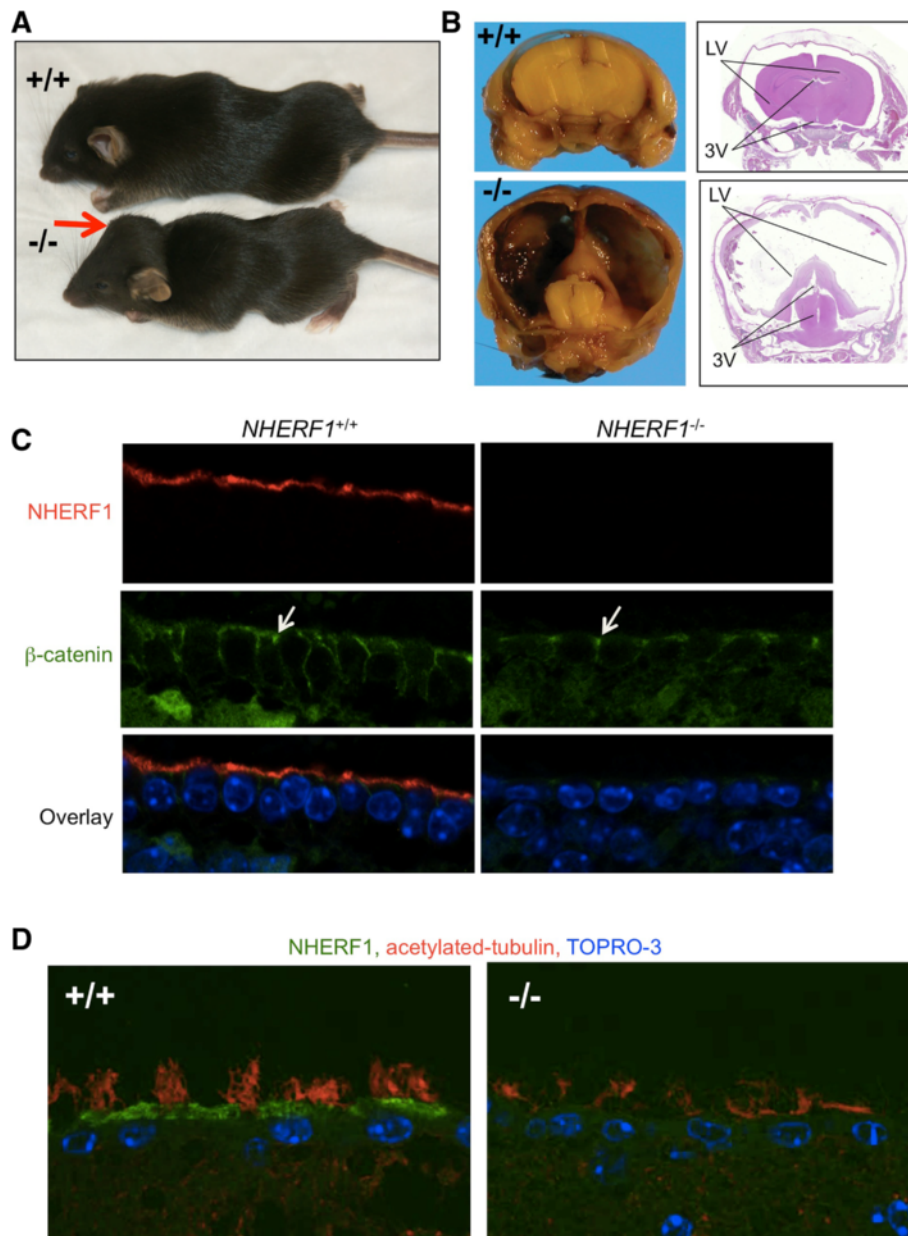


**Figure 1** *NHERF1*-deficient mice develop hydrocephalus. **A-B**. Comparison between 5-week-old *NHERF1*(+/+) and (-/-) littermates showing smaller size and bossed skull (arrow) (A) and severely distended 3<sup>rd</sup> (3V) and lateral ventricles (LV) with compression of the brain, resulting in a thin nutshell appearance of the cerebral hemispheres (B) in the *NHERF1*(-/-) littermate. **C**. Immunofluorescence analysis of 5-week-old *NHERF1* (+/+) mice and their *NHERF1*(-/-) littermates with subclinical mild hydrocephalus shows *NHERF1* labeling of the apical PM in *NHERF1*(+/+) ependyma and  $\beta$ -catenin labeling of adherens junctions (arrows) in both genotypes. **D**. Acetylated tubulin immunofluorescence labeling of the ependymal cilia shows robust cilia tufts in *NHERF1*(+/+) mice and present but disorganized cilia in *NHERF1*(-/-) littermates with subclinical mild hydrocephalus.

Examination of NHERF1 expression in brain sections showed that NHERF1 is most highly expressed at the apical PM of ependymal cells, followed by lower expression levels in choroid plexus cells (Additional file 1: Figure S2). Both cells types have been involved in the development of non-obstructive hydrocephalus, either through impaired cilia motion in the case of ependymal cells [3] or by hyperproduction of CSF, usually in choroid plexus hyperplasia [20]. Since we did not observe choroid plexus hyperplasia in *NHERF1*-deficient mice, we further characterized the ependymal cells. In overt hydrocephalus forms, the ependymal layer was flattened and disrupted (Additional file 1: Figure S3), most likely secondary to increased CSF pressure. In the mild forms, co-staining with NHERF1 and  $\beta$ -catenin antibodies showed only minor flattening of the ependymal layer and preservation of the lateral cell-cell adherens junctions (Figure 1C). In the latter forms, labeling of the ependymal cilia with acetylated tubulin antibody showed cilia disorganization in *NHERF1*-deficient animals as compared to the prominent tufts of cilia observed in wild-type animals (Figure 1D). These results suggested an involvement of NHERF1 in structuring the apical PM of ependymal cells by controlling cilia distribution.

### NHERF1 labels polarity membrane structures in ependymal tumors

The association between the intestinal morphogenetic function of NHERF1 in *NHERF1*-deficient mice and an oncogenic function in human colorectal cancer [9,16], suggested the possibility of a parallel association between a structural role of NHERF1 in ependymal apical PM organization and the pathogenesis of ependymal tumors. To verify this hypothesis, we confirmed that the high ependymal apical PM expression found in mouse CNS is present in human CNS (Figure 2A). We have previously shown that the NHERF1 apical PM expression from colonic epithelial cells is lost early in the progression of colorectal cancer [9]. Strikingly, in ependymal tumors NHERF1 remained prominently retained in perinuclear dot-like structures (Figure 2B) that correspond ultrastructurally to microlumens, polarized structures characteristic for neoplastic cells of ependymal origin. Microlumens are delineated by a membrane containing the same specialized structures, microvilli and occasionally cilia, as the polarized apical PM of non-neoplastic ependymal cells. Ring-like structures, deemed to be specific for ependymoma [21], and likely representing larger microlumens, were also labeled by NHERF1 (Figure 2C, arrows).

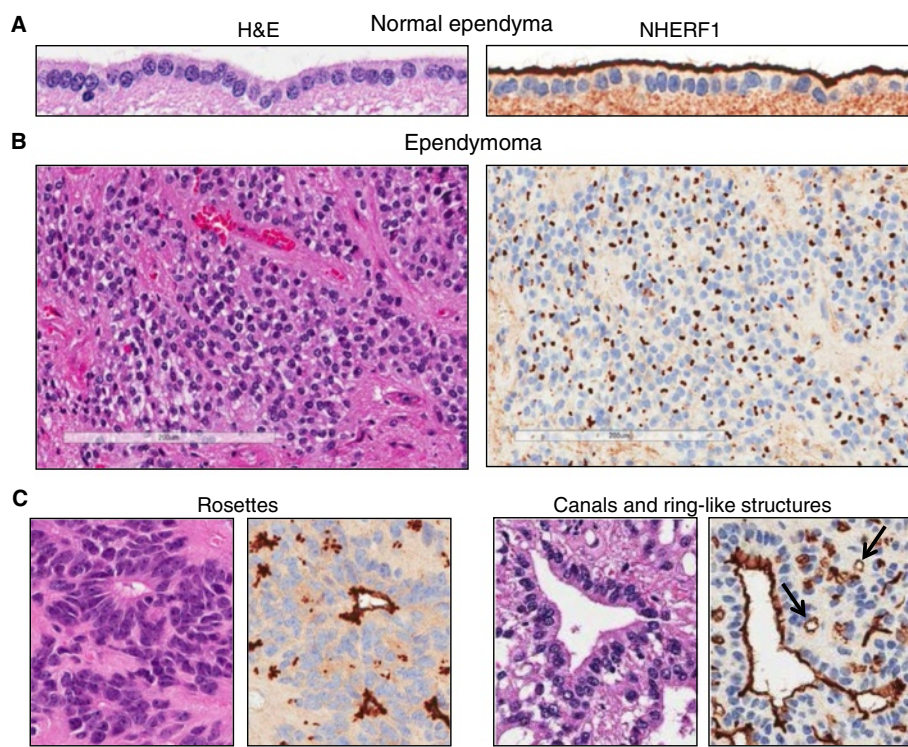


**Figure 2** NHERF1 labels polarity membrane structures in ependymoma. **A-B.** IHC with NHERF1 antibody highlights the apical PM of human normal ependyma (**A**) and microlumens in ependymoma (**B**). **C.** Serial sections from ependymoma cases stained with H & E and NHERF1 show apical PM labeling of rosettes, canals and ring-like structures (arrows) by NHERF1.

Histologically, a minority of ependymomas harbor characteristic arrangements of neoplastic cells in rosettes delimiting a lumen (“true rosettes”) or, more rarely, in canals where they mimic closely the polarized lining of the ventricles. NHERF1 labeled the apical PM of true rosettes and canals (Figure 2C), indicating that in ependymoma NHERF1 specifically labels polarized structures which include a membrane-bordered lumen.

### NHERF1 organizes protein complexes with moesin and PTEN in ependymal polarity structures

NHERF1 establishes protein complexes at the apical PM of epithelia that are essential for apico-basal polarity [12,16].

To investigate the composition of NHERF1 protein complexes in ependymoma, we screened the intracellular localization of the NHERF1 ligands moesin, NF2, PTEN, PDGFR $\alpha$ , EGFR, YAP1,  $\beta$ -catenin and PHLPP2 that have been functionally involved in primary brain tumors [11,22-27] (Figure 3A). The apical PM of normal ependyma and the various ependymoma polarity structures, including microlumens, rosettes, and canals, consistently showed PM localization of moesin, similar to NHERF1 (Figure 3B). NF2 somatic mutations are the most frequent individual gene mutations in spinal cord ependymomas, where they reach 43% [28]. NF2 IHC in normal ependymal lining and ependymomas showed only faint or no labeling of apical

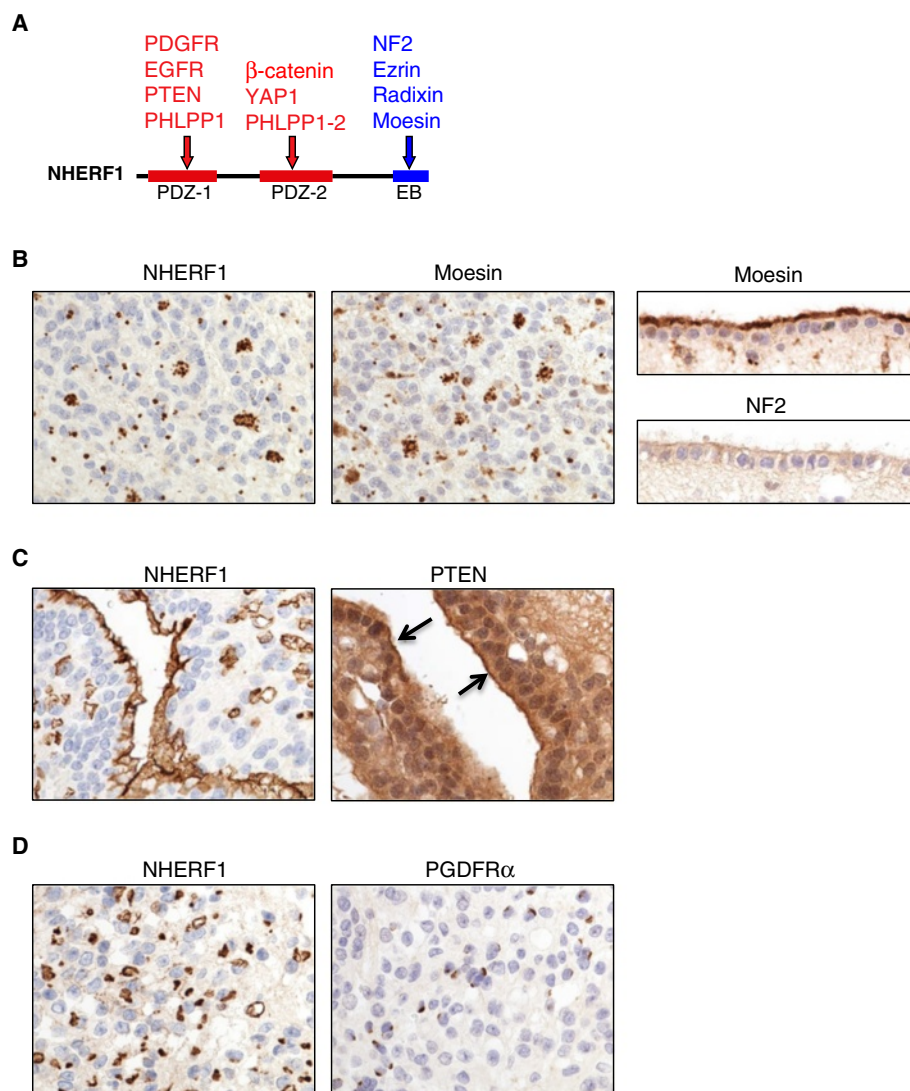


**Figure 3** NHERF1, moesin, and PTEN localize to ependymal polarized structures. **A**. Schematic NHERF1 structure shows the N-terminal PDZ domains (1 and 2) and the C-terminal ERM-binding (EB) region with selected ligands. **B**. Serial sections from an ependymoma case showing localization of NHERF1 and moesin to microlumens and rosettes. Normal ependyma shows apical PM labeling with moesin, similar to NHERF1 but not with NF2 (right panels). **C-D**. Serial sections from an ependymoma case show the apical PM of canals labeled by NHERF1 and PTEN (arrows) antibodies (C) and NHERF1 microlumens distinct from the PDGFR $\alpha$  punctate or linear perinuclear staining (D).

PM (Figure 3B), respectively, suggesting that NF2, unlike moesin, is not a major ligand of NHERF1 in these polarized structures.

Among the NHERF1 PDZ-domain ligands, PTEN was detected at the apical PM of ependymal polarity structures similar to NHERF1 (Figure 3C). The major fraction of PTEN was cytoplasmic, as previously described [12,29]. Other NHERF1 ligands, such as PDGFR $\alpha$ , localized in sparse perinuclear dot-like or cap-like structures that appeared to be distinct from the NHERF1-labeled microlumens (Figure 3C). This PDGFR $\alpha$  staining, most likely associated with the Golgi apparatus, was focal in ependymomas and was also present in the NHERF1-negative anaplastic ependymoma and anaplastic astrocytoma cases screened. EGFR was not detected in ependymoma. The NHERF1 PDZ2 domain ligands  $\beta$ -catenin and YAP1 had a strong and diffuse cytoplasmic localization (Additional file 1: Figure S4). YAP1 also displayed nuclear staining, most prominent in anaplastic ependymoma cases (not shown). Taken together, these data indicated that NHERF1 organizes complexes mainly with moesin and PTEN at the apical PM of polarized structures from ependymal neoplastic cells.

#### NHERF1 is a diagnostic marker for ependymoma

To determine whether NHERF1 can be used as a diagnostic marker of ependymal tumors, a multi-institutional effort

assembled a total of 113 primary brain tumors consisting of ependymomas, anaplastic ependymomas, and lower grade ependymal tumors, as well as miscellaneous other tumors considered in the differential diagnosis (Table 1). Although we focused our attention on the diagnosis of adult cases, smaller subsets of pediatric cases were also included for comparison. Patient demographics, as well as the localization of tumors, are presented in Table 1.

All 34 ependymoma cases in our series showed NHERF1 expression in microlumens, either in a diffuse pattern (31 of 34 cases), or more rarely, in a focal distribution (3 of 34 cases). The diffuse NHERF1 microlumen pattern was also present in 35.3% and 44.1% of cases with negative or lower epithelial membrane antigen (EMA) staining, respectively (Figure 4A and Additional file 1: Figure S5), indicating a higher sensitivity of NHERF1 for microlumen detection in ependymoma. The density of microlumens was quantified in tumors with diffuse NHERF1 expression and showed approximately 1 microlumen/2 nuclei (Figure 4B and Additional file 1: Figure S6) in the majority of the tumors. A sparse diffuse NHERF1 expression was also observed in some ependymoma cases (as in Figure 4A), with microlumen density similar to that observed in subependymoma cases. We also quantified the presence of ring-like structures and found 47% and 36.3% of ependymomas and anaplastic

**Table 1 NHERF1 in ependymal tumors and in other tumors considered in the differential diagnosis**

Diagnosis	Patients		Site	NHERF1 microlumen positivity			Total
	No. cases gender	Mean age (range)		Diffuse	Focal	Total/Site	
Ependymoma	34 <sup>1</sup>	44.6 (12 <sup>1</sup> -74)	ST: 5 <sup>1</sup>	5 (100%)		5 (100%)	34 (100%)
	20M, 14F		PF: 8	8 (100%)		8 (100%)	
			SC:21	18 (85%)	3 <sup>2</sup> (15%)	21 (100%)	
Adult Anaplastic ependymoma	9	33 (23-49)	ST: 7	2 (28%)	2 (28%)	4 (57%)	6 (67%)
	5M, 4F		PF: 1	1 (100%)	0	1 (100%)	
			SC: 1	0	1 (100%)	1 (100%)	
Pediatric Anaplastic ependymoma	5 4F, 1M	11.8 (6-17)	ST: 3	2 (67%)	1 (33%)	3 (100%)	5 (100%)
			PF: 2	2 (100%)	0	2 (100%)	
Subependymoma	6 4M, 2F	60.5 (40-68)	ST: 5 PF: 1	5 (100%) 1 (100%)	0 0	5 (100%) 1 (100%)	6 (100%)
Mixopapillary ependymoma	5 3F, 2M	45.6 (34-65)	SC: 5	0	3 (60%)	3 (60%)	3 <sup>3</sup> (60%)
Glioblastoma	15 <sup>1</sup> 7M, 8F	54.2 (12 <sup>1</sup> -76)	ST: 13 PF: 2 <sup>1</sup>	0 0	3 (23%) 0	3 (23%) 0	3 (20%)
AT/RT	2 2F	0.75 (0.4-1.1)	PF: 2	0	0	0	0%
Medulloblastoma	6 5M, 1F	24 (8-63)	PF: 6	0	0	0	0%
Diffuse gliomas <sup>4</sup>	22 16M, 6F	46.5 (27-78)	ST: 22	0	0	0	0%
Pilocytic astroc.	4 3M, 1F	31.5 (18,61)	ST:1 PF: 2 SC: 1	0	0	0	0%
Schwannoma	5 3M, 2F	46 (29-56)	PF: 4 SC: 1	0	0	0	0%

M, male; F, female; ST, supratentorial; PF, posterior fossa; SC, spinal cord.

<sup>1</sup>1 pediatric case.

<sup>2</sup>2 tanycytic and 1 giant cell ependymoma.

<sup>3</sup>All myxopapillary ependymomas had focal NHERF1 membranous staining and positive canals.

<sup>4</sup>Diffuse gliomas comprise oligodendroglioma WHO grade II (n = 5) and III (n = 1), oligoastrocytoma WHO grade II (n = 8) and III (n = 4), and astrocytoma WHO grade II (n = 1) and III (n = 3).

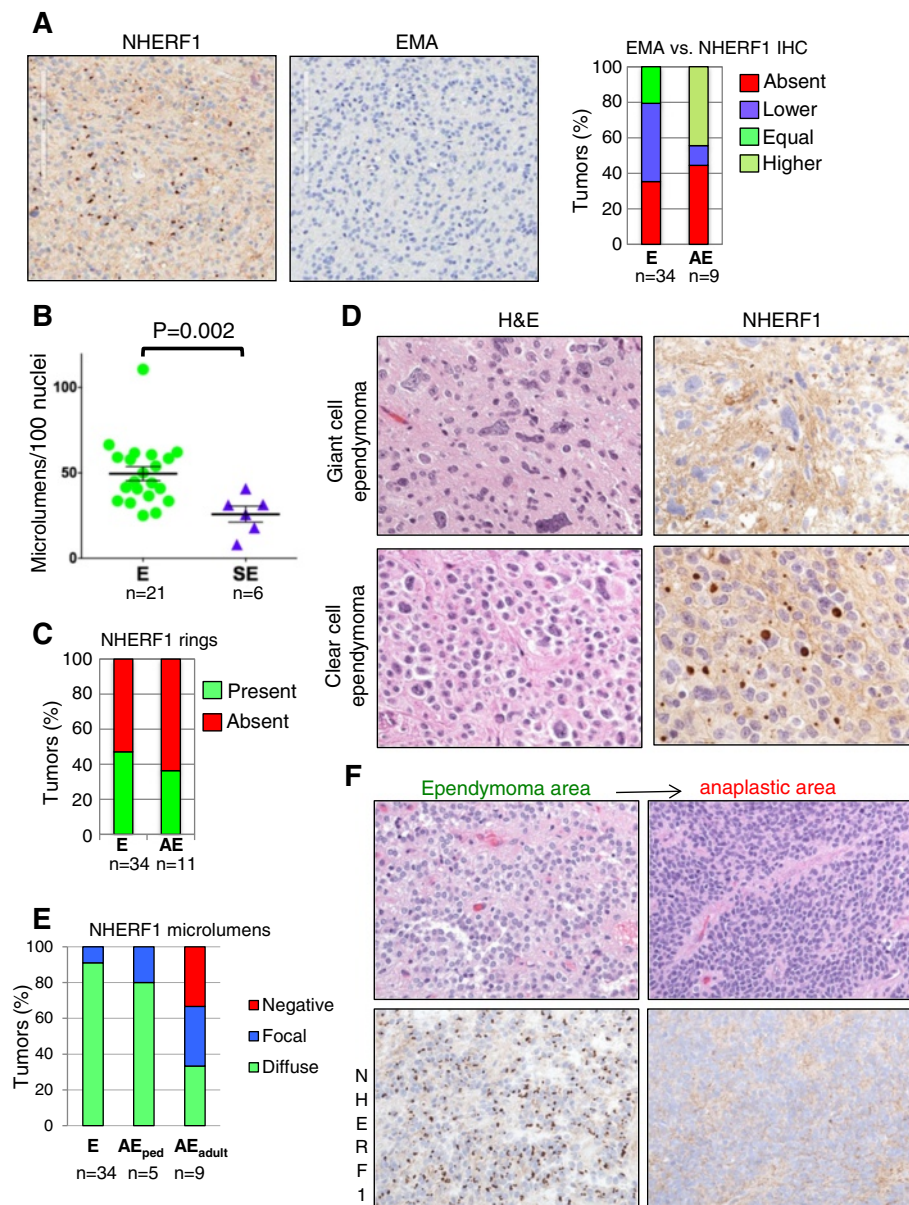


**Figure 4 NHERF1 is a marker for ependymoma.** **A.** Comparative IHC with NHERF1 and EMA antibodies on serial sections from an ependymoma case shows microlumen detection only by NHERF1. The EMA versus NHERF1 staining was similarly performed in all the ependymomas (E) and in the NHERF1-positive anaplastic ependymomas (AE), and the quantification is shown in the graph. **B.** Quantification of microlumen density in ependymal tumors. E, ependymoma; SE, subependymoma. **C.** Quantification of the ring-like structures labeled by NHERF1 in ependymoma (E) and anaplastic ependymoma (AE) tumors. **D.** IHC with NHERF1 antibody in ependymoma variants shows microlumen labeling. **E.** Extent of NHERF1 microlumen labeling in ependymoma (E), pediatric anaplastic ependymoma (AE<sub>ped</sub>) and adult anaplastic ependymoma (AE<sub>adult</sub>) illustrates significant NHERF1 loss in the latter. **F.** NHERF1 IHC of an anaplastic ependymoma case containing areas of classical ependymoma morphology (left) and areas of anaplasia (right) shows almost complete loss of NHERF1-labeled microlumens from the anaplastic component.

ependymomas, respectively, to contain these specific structures (Figure 4C). Notably, these structures were detected in only 31% of ependymomas by EMA IHC in a previous study [21]. Focal NHERF1 labeling was observed in two cases of the tanycytic ependymoma subtype, although several other tanycytic ependymomas showed diffuse NHERF1 pattern, and in one case of the

giant cell ependymoma subtype (Figure 4D). Clear cell ependymomas showed diffuse NHERF1 microlumen labeling (Figure 4D).

WHO grade I subependymomas showed sparse diffuse NHERF1 microlumen labeling in 100% of the cases, with a density of 1 microlumen/4 nuclei (Figure 4B and Additional file 1: Figure S7). Although microlumen

density was significantly lower than in ependymoma, the diffuse presence of microlumens is consistent with an ependymal origin of subependymomas.

Myxopapillary ependymomas are WHO grade I ependymal tumors with good prognosis arising with highest frequency in the cauda equina. NHERF1 labeling showed a distinctive pattern consisting mainly of canals, membranous staining, and focal areas of microlumens (Additional file 1: Figure S8 and Table 1).

Our analysis of WHO grade III anaplastic ependymomas showed a greater degree of NHERF1 expression in pediatric cases in comparison to adult tumors. NHERF1 microlumens were seen in 100% of pediatric cases, primarily with a diffuse pattern, while adult cases showed an overall 67% NHERF1 microlumen positivity with reactivity equally divided between diffuse and focal (Table 1, Figure 4E). In anaplastic tumors with foci of classical ependymoma morphology, an abrupt NHERF1 expression loss was noted in the anaplastic component of the tumor (Figure 4F and Additional file 1: Figure S9), suggesting loss of differentiation in these advanced tumors. Interestingly, EMA perinuclear reactivity was maintained in the anaplastic areas (Figure 4A graph and Additional file 1: Figure S9), reminiscent of the upregulation of EMA, a transmembrane glycoprotein also known as Mucin 1, in a series of epithelial cancers. Even if this reactivity corresponds most likely to Golgi rather than to microlumen staining, it is sometimes difficult to distinguish between these patterns. The four cases in which EMA was retained in anaplastic areas but NHERF1 was negative were scored as higher EMA (Figure 4A graph and Additional file 1: Figure S9). EMA staining was absent in four of the NHERF1-positive cases, two of which had only focal NHERF1 microlumen labeling (Figure 4A graph).

The specificity of NHERF1 microlumen pattern as diagnostic marker for ependymal tumors was assessed by screening 54 tumors of different origin that are typically considered in the differential diagnosis (Table 1). For posterior fossa pediatric tumors, medulloblastomas consistently lacked NHERF1 polarity structures and the two cases of atypical teratoid/rhabdoid tumors screened were negative as well. For adult posterior fossa and spinal cord tumors, schwannomas were negative for NHERF1 polarity structures. Similarly, NHERF1 polarity structures were absent in glial tumors such as pilocytic astrocytoma, oligodendroglioma, mixed oligoastrocytoma and anaplastic astrocytoma. Most glioblastoma cases were negative for NHERF1 microlumen labeling, however, 20% showed focal microlumen formation (Additional file 1: Figure S10). No ring-like or other polarity structures were labeled by NHERF1 in these cases.

## Discussion

The pathologic diagnosis of ependymoma is based on H&E histologic examination and confirmation of the

neoplastic origin by glial fibrillary acidic protein IHC. True ependymal rosettes and canals are obvious histologic features of ependymoma that occur in a minority of cases. Microlumens, the putative precursor of true rosettes, are more prevalent and are detected traditionally by EM. As EM is expensive, time-consuming and restricted to only few centers, EMA IHC is used routinely as an alternative to EM for microlumen detection. Unfortunately, EMA is not a reliable diagnostic tool due to its low detection sensitivity, as in our series, and to its reported decreased specificity for ependymoma [21]. We show here that NHERF1 IHC has a high sensitivity and specificity for microlumen detection in ependymal tumors, and therefore can be used reliably as a diagnostic marker in these tumors. We have also identified moesin in ependymal polarity structures, however, the low affinity of the moesin antibody and its labeling of blood vessels indicate that NHERF1 is a superior diagnostic marker. The lower grade ependymal tumors, including subependymoma and ependymoma, consistently showed NHERF1 microlumen labeling, usually with diffuse pattern. Labeling in anaplastic varied by age: all pediatric cases were NHERF1-positive, generally with diffuse reactivity, while only two-thirds of adult cases were NHERF1-positive, either diffusely or focally. The presence of areas of classical ependymoma morphology with abundant NHERF1 staining in otherwise anaplastic tumors supports the diagnosis in these advanced tumors. To our knowledge, NHERF1 IHC represents the most sensitive method for microlumen detection in ependymoma.

Due to the lack of effective chemotherapy regimens, recent efforts have been directed towards understanding the pathogenesis of ependymoma. Extensive mRNA microarray and CGH analyses showed that ependymomas are heterogenous tumors that, depending on their location –spinal, supratentorial, or in the posterior fossa - show different molecular signatures [30,31]. Interestingly, NHERF1, a marker of apical PM in normal ependyma, consistently highlighted the microlumens of ependymoma regardless of location, attesting to a common origin for these tumors. The presence of identical NHERF1-labeled microlumens in clusters of normal ependymal cells that do not line the ventricular system raises the possibility of tumor initiation from these clusters. It is thus foreseeable that the different molecular signatures result from the proliferative response of similar ependymal precursor cells to location-specific environmental cues. In this respect, it is noteworthy that defects of ciliogenesis characterize both a subset of posterior fossa ependymomas in children [31] and a series of developmental posterior fossa deficits [32,33], pointing to common molecular pathways for both posterior fossa abnormalities.

Apico-basal cell polarity is a morphological characteristic disrupted early in the development of epithelial malignancies [34]. We have previously shown that NHERF1

deficiency in mice induces structural abnormalities of the intestinal apical PM [16] that translate into defective epithelial morphogenesis with loss of apico-basal polarity and epithelial-mesenchymal transition in colorectal cancer cells [9,12]. In this study, the presence of hydrocephalus and of ependymal apical PM defects in *NHERF1*-deficient mice translated into the characterization of NHERF1-containing precursor polarized structures in ependymoma. The sensitive detection of microlumens by NHERF1 antibody revealed loss of these structures in anaplastic foci present in some WHO grade II ependymomas and a drastic reduction in adult anaplastic ependymoma, most likely due to lack of differentiation of the constituent anaplastic cells. Beside its structural role, NHERF1 has been implicated in oncogenic signaling, especially in the phosphoinositide 3-OH kinase (PI3K)-Akt and Wnt- $\beta$ -catenin pathways [10,11,27,35]. In glioblastoma, NHERF1 loss from the PM has been shown to displace PTEN from the PM and consequently activate PI3K-Akt pathway [14]. Similarly, the loss of NHERF1 and associated proteins from the PM of ependymal polarity structures in anaplastic ependymoma is prone to result in PTEN cytoplasmic displacement and activation of the PI3K-Akt pathway. Thus, in an analogous manner to other cancers [12,14,36], the regulation of morphogenesis and cell growth by NHERF1 subcellular localization emerges also in ependymal oncogenesis, with direct translation to the diagnosis of ependymal tumors.

## Additional file

**Additional file 1: Figure S1.** Subclinical hydrocephalus in *NHERF1*-deficient mice. **Figure S2.** NHERF1 expression in the CNS of mice. **Figure S3.** Disruption of the ependymal layer in *NHERF1*-deficient mice. **Figure S4.** Expression of  $\beta$ -catenin and YAP1 in ependymoma. **Figure S5.** Comparative NHERF1 and EMA labeling in ependymoma. **Figure S6.** Quantification of NHERF1 microlumen density in ependymoma. **Figure S7.** NHERF1 expression in subependymoma. **Figure S8.** NHERF1 expression in myxopapillary ependymoma. **Figure S9.** Comparative NHERF1 and EMA labeling in anaplastic ependymoma. **Figure S10.** NHERF1 expression in glioblastoma.

## Competing interests

The authors declare that they have no competing interests.

## Acknowledgements

The authors thank James Goldman for reading the manuscript and valuable comments, Charles Timmons for insightful suggestions, and Niccole Williams, Agatha Villegas and Mary Moise for administrative assistance. Funding for this work: National Institutes of Health grants NCI-CA107201 to MMG and NCI-CA16672 for animal breeding.

## Author details

<sup>1</sup>Department of Pathology, The University of Texas Southwestern Medical Center, Dallas, TX 75390, USA. <sup>2</sup>Department of Neuro-Oncology, The University of Texas MD Anderson Cancer Center, Houston, TX 77030, USA. <sup>3</sup>Department of Pathology, Vanderbilt University Medical Center, Nashville, TN 37232, USA. <sup>4</sup>Department of Pathology, Columbia University, New York, NY 10032, USA.

Received: 16 February 2015 Accepted: 18 February 2015

Published online: 08 March 2015

## References

- Del Bigio MR (2010) Ependymal cells: biology and pathology. *Acta Neuropathol* 119:55–73
- Spassky N, Merkle FT, Flames N, Tramontin AD, Garcia-Verdugo JM, Alvarez-Buylla A (2005) Adult ependymal cells are postmitotic and are derived from radial glial cells during embryogenesis. *J Neurosci* 25:10–18
- Lee L (2013) Riding the wave of ependymal cilia: genetic susceptibility to hydrocephalus in primary ciliary dyskinesia. *J Neurosci Res* 91:1117–1132
- Kilday JP, Rahman R, Dyer S et al (2009) Pediatric ependymoma: biological perspectives. *Mol Cancer Res* 7:765–786
- Iqbal MS, Lewis J (2013) An overview of the management of adult ependymomas with emphasis on relapsed disease. *Clin Oncol* 25:726–733
- Stemmer-Rachamimov AO, Wiederhold T, Nielsen GP et al (2001) NHERF, a merlin-interacting protein, is primarily expressed in luminal epithelia, proliferative endometrium, and estrogen receptor-positive breast carcinomas. *Am J Pathol* 158:57–62
- Ardura JA, Friedman PA (2011) Regulation of G protein-coupled receptor function by Na<sup>+</sup>/H<sup>+</sup> exchange regulatory factors. *Pharmacol Rev* 63:882–900
- Georgescu MM, Morales FC, Molina JR, Hayashi Y (2008) Roles of NHERF1/EBP50 in cancer. *Curr Mol Med* 8:459–468
- Hayashi Y, Molina JR, Hamilton SR, Georgescu MM (2010) NHERF1/EBP50 is a new marker in colorectal cancer. *Neoplasia* 12:1013–1022
- Kreimann EL, Morales FC, de Orbeta-Cruz J et al (2007) Cortical stabilization of beta-catenin contributes to NHERF1/EBP50 tumor suppressor function. *Oncogene* 26:5290–5299
- Takahashi Y, Morales FC, Kreimann EL, Georgescu MM (2006) PTEN tumor suppressor associates with NHERF proteins to attenuate PDGF receptor signaling. *EMBO J* 25:910–920
- Georgescu MM, Cote G, Agarwal NK, White CL 3rd (2014) NHERF1/EBP50 controls morphogenesis of 3D colonic glands by stabilizing PTEN and ezrin-radixin-moesin proteins at the apical membrane. *Neoplasia* 16:365–374
- Mangia A, Chiriatti A, Bellizzi A et al (2009) Biological role of NHERF1 protein expression in breast cancer. *Histopathology* 55:600–608
- Molina JR, Morales FC, Hayashi Y, Aldape KD, Georgescu MM (2010) Loss of PTEN binding adapter protein NHERF1 from plasma membrane in glioblastoma contributes to PTEN inactivation. *Cancer Res* 70:6697–6703
- Kamiya K, Michel V, Giraudet F et al (2014) An unusually powerful mode of low-frequency sound interference due to defective hair bundles of the auditory outer hair cells. *Proc Natl Acad Sci U S A* 111:9307–9312
- Morales FC, Takahashi Y, Kreimann EL, Georgescu MM (2004) Ezrin-radixin-moesin (ERM)-binding phosphoprotein 50 organizes ERM proteins at the apical membrane of polarized epithelia. *Proc Natl Acad Sci U S A* 101:17705–17710
- Malafronte PJ, LePage EM, Hatanpaa KJ, Burns DK, White CL 3rd, Raisanen J (2014) Expression of MAP 2 by haemangioblastomas: an immunohistochemical study with implications for diagnosis. *Pathology* 46:450–451
- Morales FC, Hayashi Y, van Pelt CS, Georgescu MM (2012) NHERF1/EBP50 controls lactation by establishing basal membrane polarity complexes with prolactin receptor. *Cell Death Dis* 3:e391
- Shenolikar S, Voltz JW, Minkoff CM, Wade JB, Weinman EJ (2002) Targeted disruption of the mouse NHERF-1 gene promotes internalization of proximal tubule sodium-phosphate cotransporter type IIa and renal phosphate wasting. *Proc Natl Acad Sci U S A* 99:11470–11475
- Aziz AA, Coleman L, Morokoff A, Maixner W (2005) Diffuse choroid plexus hyperplasia: an under-diagnosed cause of hydrocephalus in children? *Pediatr Radiol* 35:815–818
- Hasselblatt M, Paulus W (2003) Sensitivity and specificity of epithelial membrane antigen staining patterns in ependymomas. *Acta Neuropathol* 106:385–388
- Lazar CS, Cresson CM, Lauffenburger DA, Gill GN (2004) The Na<sup>+</sup>/H<sup>+</sup> exchanger regulatory factor stabilizes epidermal growth factor receptors at the cell surface. *Mol Biol Cell* 15:5470–5480
- Maudsley S, Zamah AM, Rahman N et al (2000) Platelet-derived growth factor receptor association with Na<sup>+</sup>/H<sup>+</sup> exchanger regulatory factor potentiates receptor activity. *Mol Cell Biol* 20:8352–8363
- Mohler PJ, Kreda SM, Boucher RC, Sudol M, Stutts MJ, Milgram SL (1999) Yes-associated protein 65 localizes p62(c-Yes) to the apical compartment of airway epithelia by association with EBP50. *J Cell Biol* 147:879–890

25. Molina JR, Agarwal NK, Morales FC et al (2012) PTEN, NHERF1 and PHLPP form a tumor suppressor network that is disabled in glioblastoma. *Oncogene* 31:1264–1274
26. Reczek D, Berryman M, Bretscher A (1997) Identification of EBP50: A PDZ-containing phosphoprotein that associates with members of the ezrin-radixin-moesin family. *J Cell Biol* 139:169–179
27. Shibata T, Chuma M, Kokubu A, Sakamoto M, Hirohashi S (2003) EBP50, a beta-catenin-associating protein, enhances Wnt signaling and is over-expressed in hepatocellular carcinoma. *Hepatology* 38:178–186
28. Ebert C, von Haken M, Meyer-Puttlitz B et al (1999) Molecular genetic analysis of ependymal tumors. NF2 mutations and chromosome 22q loss occur preferentially in intramedullary spinal ependymomas. *Am J Pathol* 155:627–632
29. Martin-Belmonte F, Gassama A, Datta A et al (2007) PTEN-mediated apical segregation of phosphoinositides controls epithelial morphogenesis through Cdc42. *Cell* 128:383–397
30. Taylor MD, Poppleton H, Fuller C et al (2005) Radial glia cells are candidate stem cells of ependymoma. *Cancer Cell* 8:323–335
31. Witt H, Mack SC, Ryzhova M et al (2011) Delineation of two clinically and molecularly distinct subgroups of posterior fossa ependymoma. *Cancer Cell* 20:143–157
32. Lee JE, Gleeson JG (2011) Cilia in the nervous system: linking cilia function and neurodevelopmental disorders. *Curr Opin Neurol* 24:98–105
33. Yuan S, Sun Z (2013) Expanding horizons: ciliary proteins reach beyond cilia. *Annu Rev Genet* 47:353–376
34. Mullin JM (2004) Epithelial barriers, compartmentation, and cancer. *Sci STKE* (216):pe2
35. Lin YY, Hsu YH, Huang HY et al (2012) Aberrant nuclear localization of EBP50 promotes colorectal carcinogenesis in xenotransplanted mice by modulating TCF-1 and beta-catenin interactions. *J Clin Invest* 122:1881–1894
36. Saponaro C, Malfettone A, Dell'Endice TS et al (2014) The prognostic value of the Na(+)/H(+) exchanger regulatory factor 1 (NHERF1) protein in cancer. *Cancer Biomark* 14:177–184

**Submit your next manuscript to BioMed Central and take full advantage of:**

- Convenient online submission
- Thorough peer review
- No space constraints or color figure charges
- Immediate publication on acceptance
- Inclusion in PubMed, CAS, Scopus and Google Scholar
- Research which is freely available for redistribution

Submit your manuscript at  
[www.biomedcentral.com/submit](http://www.biomedcentral.com/submit)

